UNIVERSITY OF AMSTERDAM

UvA-DARE (Digital Academic Repository)

Dynamical and structural self-organization : a study of friction, liquid-crystal nucleus growth, and supramolecular polymers through simple models

Huisman, B.A.H.

Publication date
2008

Link to publication

Citation for published version (APA):
Huisman, B. A. H. (2008). *Dynamical and structural self-organization : a study of friction, liquid-crystal nucleus growth, and supramolecular polymers through simple models*. [Thesis, fully internal, Universiteit van Amsterdam].

General rights
It is not permitted to download or to forward/distribute the text or part of it without the consent of the author(s) and/or copyright holder(s), other than for strictly personal, individual use, unless the work is under an open content license (like Creative Commons).

Disclaimer/Complaints regulations
If you believe that digital publication of certain material infringes any of your rights or (privacy) interests, please let the Library know, stating your reasons. In case of a legitimate complaint, the Library will make the material inaccessible and/or remove it from the website. Please Ask the Library: https://uba.uva.nl/en/contact, or a letter to: Library of the University of Amsterdam, Secretariat, P.O. Box 19185, 1000 GD Amsterdam, The Netherlands. You will be contacted as soon as possible.

UvA-DARE is a service provided by the library of the University of Amsterdam (https://dare.uva.nl)
Download date:15 Nov 2026

We report Monte Carlo simulations of the self-assembly of supramolecular polymers based on a model of patchy particles. We find a first-order phase transition, characterized by hysteresis and nucleation, toward a solid bundle of polymers, of length much greater than the average gas phase length. We argue that the bundling transition is the supramolecular equivalent of the sublimation transition, which results from a weak chain-chain interaction. We provide a qualitative equation of state that gives physical insight beyond the specific values of the parameters used in our simulations.*

8

Phase transition to bundles of flexible fibers

* The body of this chapter has been published as:
B. A. H. Huisman, P. G. Bolhuis and A. Fasolino.
Phys. Rev. Lett. **100**, 188301 (2008). Appendices 8.A to 8.D are added here as supplementary material.

Self-assembly is an active field of research, driven by the desire to design new materials. Understanding the rules of self-assembly has been defined as the challenge for chemistry of this century[1]. The large molecules involved in self-assembly spontaneously organize because of highly specific interactions like hydrophobic/hydrophilic, hydrogen bonding, and $\pi - \pi$-stacking. Modeling these self-assembly processes using coarse-grained models, such as the patchy particle[2], has the potential to yield theoretical insight. Up to now, patchy-particle models have mostly been used to describe the self-assembly of functionalized colloids for photonic crystals[3], and to study the formation of self-assembled clusters[4].

We focus on linear supramolecular self-organization, like the experimentally observed reversible aggregation of discotic molecules into supramolecular polymers[5; 6; 7]. Sciortino et al.[2] showed that the Wertheim Thermodynamic Perturbation Theory (WTPT) of associating liquids accurately predicts the chain-length distribution by comparing the WTPT to simulations of square-well patchy particles. One step beyond linear polymerization is the bundling of supramolecular chains [5; 6; 7], that neither the WTPT, nor the square-well patchy particle, can deal with, since it requires chain-chain interactions.

In this chapter we present Monte Carlo simulations of patchy particles that, by decreasing temperature or increasing density first polymerize into chains and subsequently undergo a phase transition toward bundles of these chains. We interpret this bundling as a sublimation transition from a polymer gas to a solid bundle. This sub-

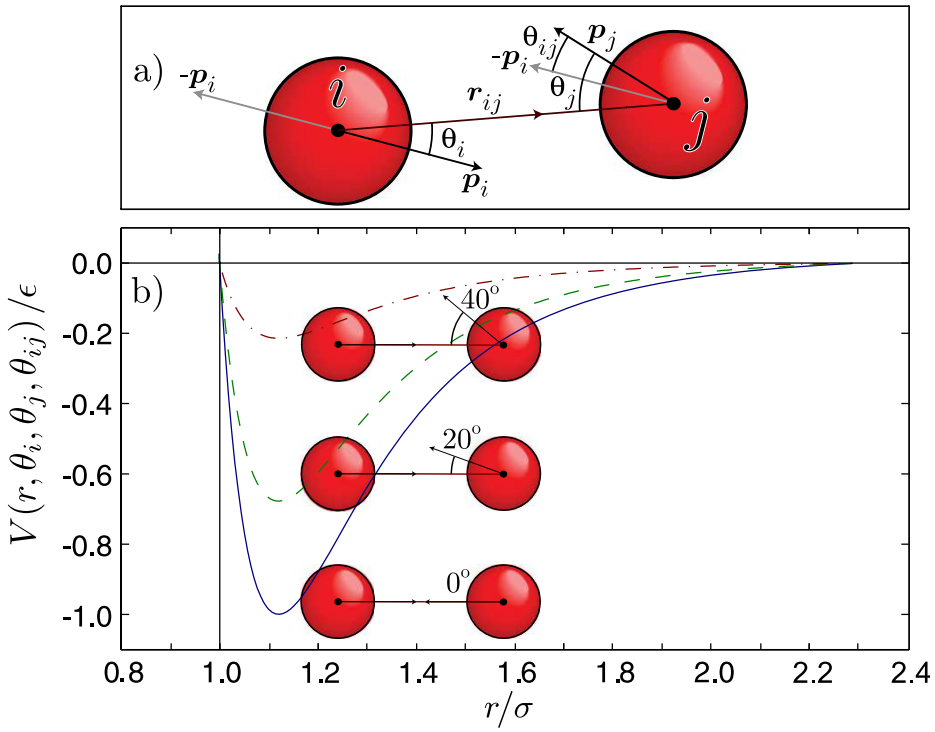

Figure 8.1: a) Geometry of the patches. θ_i is the angle between the direction $\vec{p}_i$ of patch i and the interparticle vector $\vec{r}_{ij} = \vec{r}_j - \vec{r}_i$. θ_j is the angle between the direction $\vec{p}_j$ of patch j and $\vec{r_{ji}} = -\vec{r_{ij}}$. θ_{ij} is the angle between $\vec{p}_j$ and $-\vec{p}_i$. b) Patch potential for three values of θ_j for $w = 0.4$. The strongest attraction occurs for $\theta_i = \theta_j = \theta_{ij} = 0$ and decreases rapidly for increasing angles. Particles are depicted at half their size.

limation competes with polymerization and gives rise to nontrivial phase behavior. We propose a simple thermodynamic model to describe the transition.

Our coarse-grained model of disklike molecules consists of hard spheres of diameter σ, dressed by two opposing patches. The orientation-dependent patch potential allows not only chain formation, but also exhibits a weak chain-chain interaction. The potential between patch i directed along the vector $\vec{p}_i$ and patch j along $\vec{p}_j$, illustrated in Fig. 8.1, is given by a Lennard-Jones potential of the interparticle distance $r = |\vec{r}_{ij}|$ modulated by three directional components

$$V(r,\theta_i,\theta_j,\theta_{ij}) = 4\epsilon\left[\left(\frac{\sigma}{r}\right)^{12} - \left(\frac{\sigma}{r}\right)^{6}\right]\exp\left[-\frac{\theta_i^2+\theta_j^2+\theta_{ij}^2}{4w^2}\right] \tag{8.1}$$

where ϵ is the maximum energy of interaction, and w penalizes nonperfect alignment. We truncate $V(r)$ of Eq. 8.1 at $r_c = 2.3\sigma$ and shift and rescale it to have $V(r_c) = 0$ and $V(2^{1/6}\sigma) = -\epsilon$. The first two directional components favor minimization of the angle θ_i between the patch direction $\vec{p}_i$ of patch i and the interparticle vector $\vec{r}_{ij}$, and of the angle θ_j between $\vec{p}_j$ and $\vec{r}_{ji} = -\vec{r}_{ij}$. The third component minimizes the angle

θ_{ij} between $\vec{p}_j$ and $-\vec{p}_i$, favoring parallel alignment of the patches. This potential has three advantages compared to a square-well patch potential[2]. First, it allows multiple bonds without increasing the energy per interaction site in discrete steps. This feature introduces a slight interaction between molecules in neighboring chains. Second, the desired parallel alignment of neighboring patches prevents branching (and therefore network formation) of the polymers. Finally, it allows us to tune the flexibility of a supramolecular chain. One can show that w is a measure of the chain flexibility, by calculating the bending rigidity κ, and hence the persistence length l_p of a chain [8]

$$E_{\text{bend}} = \frac{\kappa}{2}\int_0^L \frac{1}{R(s)^2}ds \;\Rightarrow\; \kappa = 2^{\frac{1}{6}}\frac{3\sigma\epsilon}{4w^2}, \text{ and } l_p \equiv \beta\kappa$$

where $\beta = (k_B T)^{-1}$, L is the chain length, and $R(s)$ is the chain radius at s. For example, the oligo(p-phenylenevinylene)-derivative OPV-4 in dodecane has $l_p = 150$nm at 300K, a molecule separation $\sigma = 0.35$nm and a bonding energy 56kJ/mol[6] yielding $w \approx 0.2$.

We study M patchy particles in a periodically repeated simulation box of volume V at temperature T by Monte Carlo simulations. The system is equilibrated by performing moves and rotations of single molecules, and of whole chains as well as reptation moves. We can simulate a limited temperature range ($k_B T \gtrsim 0.04\epsilon$) as at lower temperatures the probability of removing a molecule from a chain by a simple Monte Carlo move vanishes. We choose to consider molecules bonded if their interaction $V < -0.3\epsilon$. Contrary to the square-well patch potential [2], the potential of Eq.8.1 makes the average energy per bond E_{bond} temperature dependent. We find that equipartition (i.e. $E_{\text{bond}} = -\epsilon + 3k_B T$, independent of w) applies up to $k_B T \lesssim 0.07\epsilon$, where $E_{\text{bond}} \approx -0.79\epsilon$.

Supramolecular polymerization is reversible and there exists an equilibrium density ρ_N of chains with length N, with $N = 1, 2, \ldots, \infty$. The total density is given by $\rho = \sum_{N=1}^{\infty} N\rho_N$. The average chain length $\bar{N}$, the aggregation fraction η[9], and the fraction of unbonded sites[2] are defined as

$$\bar{N} \equiv \frac{\sum_{N=1}^{\infty} N\rho_N}{\sum_{N=1}^{\infty} \rho_N} = \frac{1}{X},\; \eta \equiv \frac{\sum_{N=2}^{\infty} N\rho_N}{\sum_{N=1}^{\infty} N\rho_N} = 1 - \frac{1}{\bar{N}^2} \tag{8.2}$$

In the ideal free-association (IFA) model[9] each bond has energy ϵ and the polymers form an ideal gas so that $\rho_N \sim \rho_1^N$

$$\bar{N} = \frac{1}{2} + \frac{1}{2}\sqrt{1 + 8\rho\Delta}, \text{ with } \Delta = \frac{v}{2}\exp(\beta G) \tag{8.3}$$

where $G \lesssim \epsilon$ is an effective free energy per bond and v is the available bonding volume per particle. Both parameters are not known a priori, and are usually fit to the average chain lengths, determined by e.g. circular dichroism measurements[6]. The WTPT includes the spatial extension of the molecules [10] neglected in the IFA-model, by calculating a reference hard sphere free energy and adding the attractive contribution

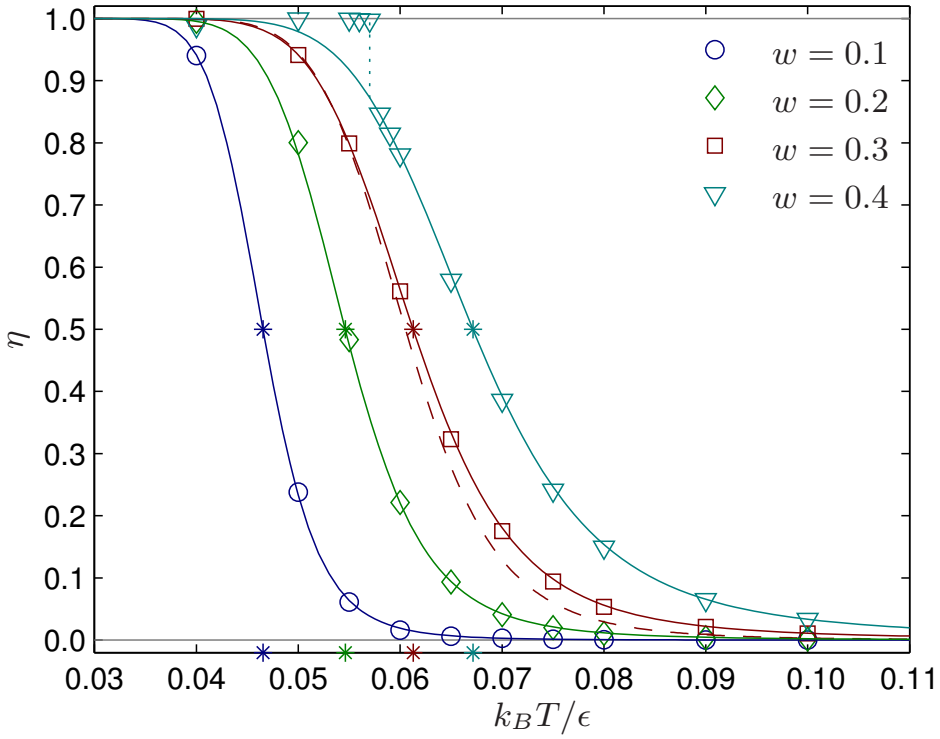

Figure 8.2: Temperature dependence of the aggregation fraction η (Eq. 8.2) for several values of the flexibility w for $M = 1330$, $\rho = 1.13 \cdot 10^{-3}\sigma^{-3}$. $\eta = 1/2$ defines the polymerization temperature T^*, indicated by an asterisk on the curves and on the horizontal axis. At $w = 0.4$ a transition from a gas of chains, to a solid bundle at $k_BT = 0.057\epsilon$ is indicated by the dotted line. Symbols denote simulation results, solid lines are the WTPT. The dashed line is a fit of the IFA-model to the curve of $w = 0.3$, with $v = 1.4 \cdot 10^{-4}\sigma^3$ and $G = 0.91\epsilon$.

of the pair potential $V_{\text{att}}(r)$. WTPT also assumes that only one interaction per attractive site is possible. The average chain length predicted by the WTPT is given by Eq. 8.3, with $\Delta = \Delta^W$

$$\Delta^{\text{W}} \equiv 4\pi \int g_{\text{rep}}(r) \left\langle \exp(-\beta V_{\text{att}}(r)) - 1 \right\rangle_{\omega_1,\omega_2} r^2 dr, \tag{8.4}$$

where Δ^{W} involves a single site-site interaction, and is related to the second virial coefficient[2], $\langle . \rangle_{\omega_1,\omega_2}$ denotes an average over all orientations ω_1 and ω_2 of the two molecules, and $g_{\text{rep}}(r)$ is the pair correlation function of the hard-sphere part of the potential. At low densities and temperatures the IFA-model and the WTPT are equivalent, and for square-well patchy particles, G becomes the well depth and v is calculated analytically [2].

In Figure 2 we compare the aggregation fraction η as a function of temperature T for several values of the flexibility w to the prediction of the WTPT with $g_{\text{rep}}(r) = 1$, appropriate at low densities, and Δ^{W} (Eq. 8.4) numerically calculated. The remark-

able agreement with simulations shows that the WTPT also holds for smoothly varying potentials on a hard sphere. We also show a fit of the IFA-model, that deviates at higher temperatures due to the temperature dependence of the association energy. We find (not shown) that this deviation reduces with decreasing w, and is negligible for $w < 0.1$. The polymerization temperature T^* is defined as the temperature where half of the molecules has aggregated, i.e. where $\eta(T^*) = \frac{1}{2}$. T^* increases with w due to an increase in available bonding volume v, or, equivalently, because a transition from an unbound to a bound state costs less entropy for a more flexible chain. For $w = 0.4$ and $k_BT < 0.058\epsilon$ a sudden jump to $\eta \approx 1$ occurs. The chains have bundled, with a concomitant increase of the average chain length and a strong depletion of the gas density. Such a sudden increase of η , not accounted for by polymerization theory, has recently been observed for the OPV-4 molecule[6].

By analyzing the radial distribution function and visual inspection, we find the bundles to have an approximate FCC structure with the bundle long axis along the 110. The crystal is not exactly FCC because it is slightly elongated along the bundle axis and contains defects. We also observe that the bundle diameter increases with density, which makes it unlikely that this patchy-particle model describes bundles of fixed finite thickness. However, we observe that thick bundles with a perfect crystal structure evolve towards prolate ellipsoids, with a much smaller aspect ratio than found growing from a polymer gas in our simulations. We believe that the long bundles we observe correspond to metastable structures resulting from kinetic growth pathways that prefer formation of long bundles, since sideways growth is only possible by a surface nucleation event, or the association of polymer chains. The latter are increasingly rare, primarily due to the finite number of particles in the simulation box. The equilibrium crystal shape might be reached faster e.g. by simulating in the grand canonical ensemble and/or by using smart Monte Carlo moves. However, the observed metastable structures might become the true equilibrium structure in the presence of chirality or larger strain in the model, as proposed in Ref. [11].

Now we examine the bundling transition in more detail. Figs. 3a and 3b show the dramatic difference between a bundled and a polymer gas configuration, while the temperatures differ by only $k_B\Delta T = 0.01\epsilon$. In the bundle the individual chains remain identifiable, with no connections between chains. Visual inspection of the process of bundling, shows that when three chains come together, they remain bonded and suddenly grow in length, suggesting a nucleation mechanism. In Fig. 3c, the bundling transition is visible as a sharp jump of the average chain length $\bar{N}(T)$. The dashed line represents systems heated up from a bundled configuration at $k_BT = 0.057\epsilon$. This hysteresis together with the nucleation mechanism, is evidence for a first-order phase transition. We identify the bundling temperature T_b at the high end of the hysteresis-loop, at $k_BT_b \approx 0.065\epsilon$. In the inset of Fig. 3c we show $\bar{N}(T)$ for several values of w. Although a stiffer chain loses less entropy upon bundling than a flexible one, T_b increases with flexibility w, similar to T^*. The transition is thus not driven by entropy, but by the interaction energy of neighboring chains (Eq. 8.1)

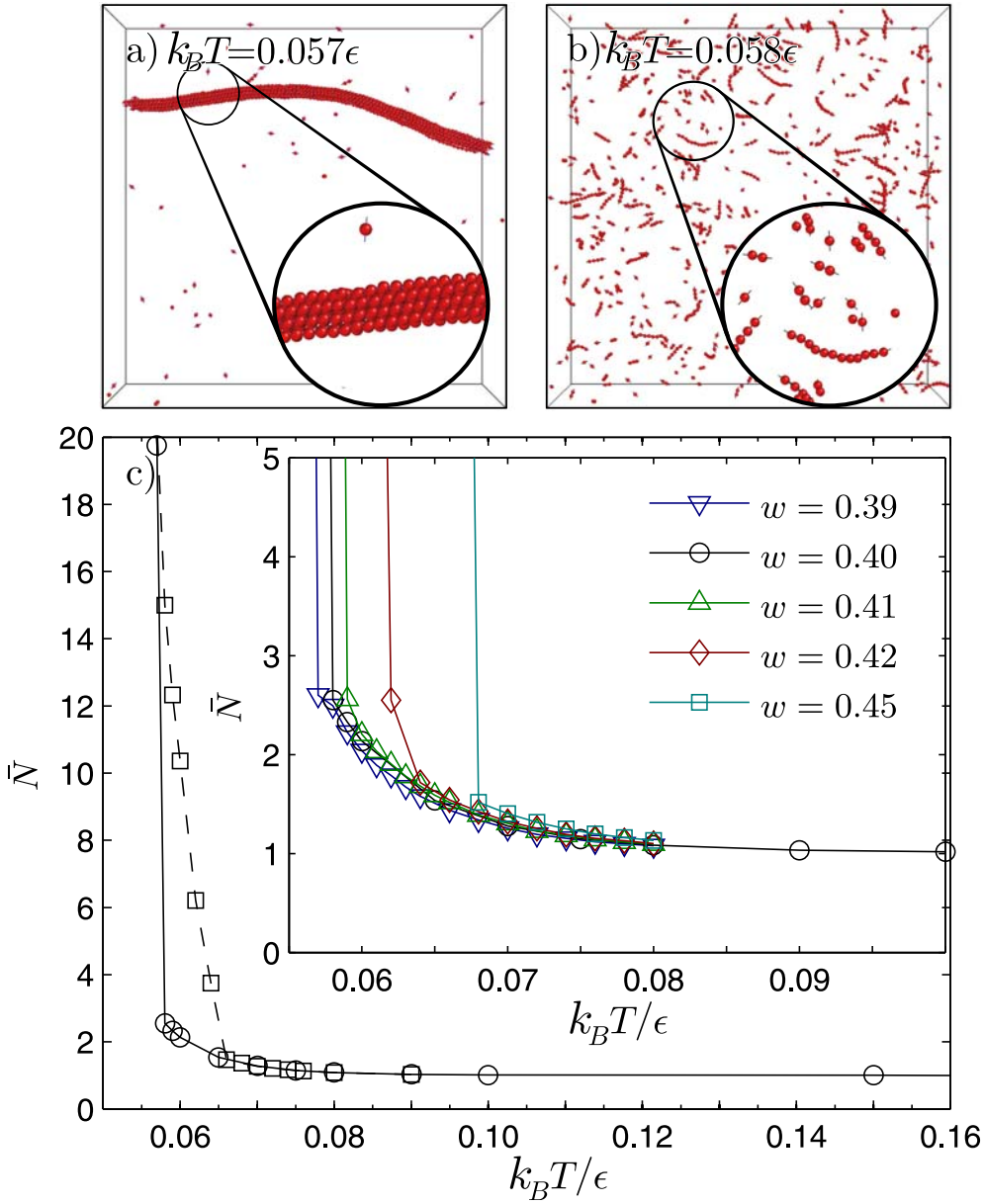

Figure 8.3: Top: representative configuration for $w = 0.4$ at two very close temperatures. M, ρ as in Fig. 2. a) $k_BT = 0.057\epsilon$, where a solid bundle has nucleated. b) $k_BT = 0.058\epsilon$ where the system is still a polymer gas. c) Average chain length $\bar{N}(T)$ for $w = 0.4$. The solid line shows the jump of $\bar{N}$ for $k_BT \approx 0.057\epsilon$ on cooling. The dashed line shows the hysteresis while raising T from an equilibrated system initially at $k_BT = 0.057\epsilon$. Inset: Same curve for several values of w. No hysteresis loop is shown. Notice that the bundling temperature increases with w.

that, at large θ, increases with w. Assuming the patches in neighboring chains to be perfectly aligned, the smallest angle θ_i between molecules in neighboring chains is $\theta_i \sim \arctan(2^{-\frac{1}{6}}) \approx 0.73\text{rad}$ or $42°$. For $w \lesssim 0.15$ this lateral interaction is negligible ($\theta_i/2w \approx 2.4$). Increasing w also increases the available lateral bonding volume, decreasing the entropy loss upon bundling.

We interpret the bundling as a sublimation transition, from a polymer gas to a solid bundle. To derive an approximate equation of state, we equate the chemical potential μ_{sol} of a bundle to that of a polymer gas μ^{p}. By using the IFA-model we can derive

$$\mu^{\text{p}} = \frac{\partial F}{\partial M} = \mu^{\text{m}} - \frac{2}{\beta} \ln \bar{N}, \text{ with } \mu^{\text{m}} = \frac{1}{\beta} \ln \left[\frac{v\rho}{Z_1} \right] \tag{8.5}$$

where μ^{m} is the chemical potential of an ideal gas of monomers with internal partition function Z_1, and where $\bar{N}$ is given either by the IFA-model (Eq. 8.3), or by the WTPT (Eqs. 8.3 and 8.4). For our rigid molecules, $Z_1 = 1$. We then model the bundle by an Einstein crystal[12] with

$$\mu_{\text{sol}} = -\epsilon_{\text{sol}} + \frac{1}{\beta} \ln \left[\Lambda^3 \left(\frac{\beta k}{2\pi} \right)^{\frac{3}{2}} \right] \tag{8.6}$$

where ϵ_{sol} and k are the equilibrium energy, and the spring constant of the Einstein crystal, respectively. We replace the de Broglie wavelength term with the bonding volume $\Lambda^3 = v$, as was done to derive the IFA-model. Equating μ^{m} of Eq. 8.5 to μ_{sol} of Eq. 8.6 results in the sublimation line of an ideal gas of monomers $\rho^{\text{m}}_{\text{sub}}$

$$\rho^{\text{m}}_{\text{sub}} = \left(\frac{\beta k}{2\pi} \right)^{\frac{3}{2}} \exp(-\beta \epsilon_{\text{sol}}) \tag{8.7}$$

Solving $\mu^{\text{p}} = \mu_{\text{sol}}$ yields the sublimation density for the polymer gas $\rho^{\text{p}}_{\text{sub}}$

$$\rho^{\text{p}}_{\text{sub}} = \frac{\rho^{\text{m}}_{\text{sub}}}{\left(2\rho^{\text{m}}_{\text{sub}}\Delta - 1\right)^2}. \tag{8.8}$$

It is useful to define the density at the polymerization temperature $\rho^* = \rho(T^*)$, by combining Eqs. 8.2 and 8.3

$$\eta(T^*) = \frac{1}{2} \quad \Rightarrow \quad \rho^* = \frac{2 - \sqrt{2}}{2\Delta}. \tag{8.9}$$

Comparison of $\rho^{\text{p}}_{\text{sub}}$ to ρ^* allows us to estimate whether the sublimation transition is dominated by the bundling of polymers (Eq. 8.8), or of monomers (Eq. 8.7).

In Fig. 4, we compare the $T - \rho$ phase diagram resulting from our simulations to the theoretical polymerization and sublimation line. The parameters of the Einstein crystal were determined by fitting Eq. 8.8 to our simulations, with $\Delta = \Delta^{\text{W}}$ of Eq. 8.4, and the polymerization density ρ^* calculated from the WTPT. At low densities $\rho^{\text{p}}_{\text{sub}} \sim$

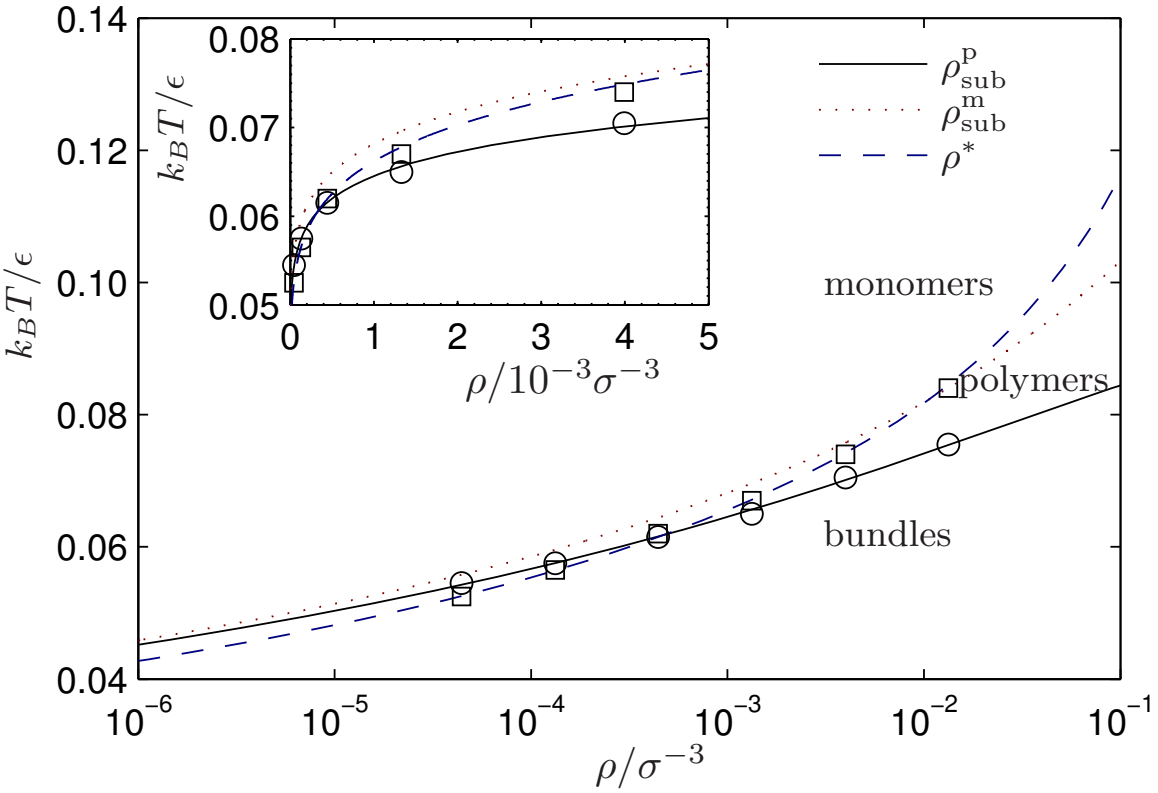

Figure 8.4: Simulated gas-solid coexistence line (circles), and polymerization line (squares) for $w = 0.4$, together with the theoretical monomer sublimation line $\rho^{\rm m}_{\rm sub}$ (Eq. 8.7, dotted line), polymer sublimation line $\rho^{\rm p}_{\rm sub}$ (Eq. 8.8, solid line), and polymerization line ρ^* (Eq. 8.9, dashed line) based on the WTPT-description of a polymer gas in equilibrium with an Einstein crystal, with $k = 1.2 \cdot 10^3 \epsilon\sigma^{-2}$ and $\epsilon_{\rm sol} = 1.05$. In the inset we show the same, but on a linear density scale.

$\rho^{\rm m}_{\rm sub}$, since the polymerization temperature is lower than the sublimation temperature, i.e. $T^* < T_b$. The sublimation lines differ at higher densities, because $\mu^{\rm p}$ tends to a finite value, whereas the chemical potential of an ideal monomer gas tends to zero. The average polymer length $\bar{N}$ at the sublimation transition increases for decreasing w. When the lateral interactions vanish ($w < 0.15$), the bundling transition would occur for infinitely long polymers. The agreement between $\rho^{\rm p}_{\rm sub}$ and our simulations suggests that this approximate theory describes the essential physics of our patchy-particle model.

In summary, we have presented a patchy-particle model that describes supramolecular polymerization and displays a first-order phase transition to bundles, due to weak chain-chain interactions. The chain-to-bundle transition can be seen as a sublimation transition from a polymer gas to a solid bundle, for which we have given a qualitative equation of state. We have related the occurrence of the phase transition

to the polymer flexibility. Our simulations show that bundling leads to a sudden increase of the average length of the aggregates. From the simulations, it is unlikely that these simple patchy particles can describe fibers with an intrinsically limited thickness. However, we believe that the patchy particle is a powerful tool for efficient modeling of complex, self-assembling systems, that can be improved by including more specific, e.g. chiral, chain-chain interactions, which might lead to bundles with fixed finite thickness.

Supplementary material

Appendix 8.A Equilibrium polymerization

In this appendix we will derive all thermodynamic properties of the ideal free-association (IFA) model, used in this chapter as a starting point to create a qualitative phase diagram of polymer sublimation. In the IFA-model each particle has two active bonding sites, and each bond lowers the energy by a constant value ϵ. It assumes that the polymers do not interact with each other, and that polymers of length N behave like an ideal gas, in equilibrium with ideal gasses of polymers of different lengths. In the limit of high temperatures and low densities, the IFA-model results in an ideal gas of monomers. The Wertheim Thermodynamic Perturbation Theory (WTPT), when applied to equilibrium polymerization, can be viewed as a nonideal gas expansion of the IFA-model, that takes the extended geometry of the molecules and their interactions into account in a similar way as done to calculate the second virial coefficient for nonideal gasses.

8.A.1 The partition function and the free energy

In a volume V an ideal gas of n_1 monomers is in equilibrium with ideal gasses of n_N polymers of length N, which we will call N-mers. The total number of particles in our volume is M, and the total particle density is $\rho = M/V$

$$M = \sum_{N=1}^{\infty} n_N N = V\rho = V \sum_{N=1}^{\infty} N\rho_N \tag{8.10}$$

where ρ_N is the density of N-mers. The partition function Q_1 of an ideal gas of monomers is given by

$$Q_1 = Z_1^{\mathrm{id}} Z_1^{n_1} = \frac{1}{n_1!}\left(\frac{V}{\Lambda^3}\right)^{n_1} Z_1^{n_1} \tag{8.11}$$

where Λ is the de Broglie wavelength. We will assume that $v = \Lambda^3$, and identify this volume with the volume available for bonding per particle. Z_1^{id} is the partition function of an ideal gas of point particles and Z_1 is the internal partition function of a single particle. The partition function of an N-mer is analogously defined as

$$Q_N = Z_N^{\mathrm{id}} Z_N^{n_N} = \frac{1}{n_N!}\left(\frac{V}{v}\right)^{n_N} Z_N^{n_N} \tag{8.12}$$

where Z_N is the internal partition function of a single N-mer. This partition function not only takes the internal freedom of the particles into account, but also the freedom and size of the polymer chain.

We assume that none of the polymers interact, so that we can write the total partition function as the product of all the N-mer partition functions

$$Q = \prod_{N=1}^{\infty} Q_N \tag{8.13}$$

The free energy F is defined by

$$F = U - TS = -\frac{1}{\beta} \ln Q = -\frac{1}{\beta} \ln \left(\prod_{N=1}^{\infty} Q_N \right) = -\frac{1}{\beta} \sum_{N=1}^{\infty} \ln Q_N \tag{8.14}$$

with $\beta^{-1} = k_B T$. The logarithm of the partition function Q_N is

$$\begin{aligned} \ln Q_N &= \ln \left(\frac{1}{n_N!} \right) + \ln \left(\frac{V}{v} \right)^{n_N} + \ln \left(Z_N^{n_N} \right) \\ &= -\ln(n_N!) - n_N \ln \left(\frac{v}{V} \right) + n_N \ln Z_N \end{aligned} \tag{8.15}$$

and using Stirling's approximation $\ln(n!) \approx n \ln(n) - n$ we get

$$\ln Q_N \approx -n_N \ln n_N + n_N - n_N \ln \left(\frac{v}{V} \right) + n_N \ln Z_N, \tag{8.16}$$

$$= n_N \left[1 - \ln \left(\frac{n_N v}{V} \right) + \ln Z_N \right]. \tag{8.17}$$

By substituting $n_N = V \rho_N$, Eq. 8.17 becomes

$$\ln Q_N = V \rho_N \left[1 - \ln \rho_N v + \ln Z_N \right] \tag{8.18}$$

Substituting Eqs. 8.18 in 8.14 gives

$$F = \frac{V}{\beta} \sum_{N=1}^{\infty} \rho_N \left[\ln \rho_N v - \ln Z_N - 1 \right] \tag{8.19}$$

8.A.2 The grand potential and the distribution of polymer lengths

The grand potential Ω is given by

$$\Omega = F - \mu^{\mathrm{p}} M = F - \mu^{\mathrm{p}} V \sum_{N=1}^{\infty} N \rho_N \tag{8.20}$$

where μ^{p} is the chemical potential of a single particle in the polymer gas and F is the total free energy. Substituting Eq. 8.19 in Eq. 8.20 gives

$$\begin{aligned} \frac{\beta \Omega}{V} &= \sum_{N=1}^{\infty} \rho_N \left[\ln \rho_N v - \ln Z_N - 1 \right] - \beta \sum_{N=1}^{\infty} \mu^{\mathrm{p}} \rho_N N \\ &= \sum_{N=1}^{\infty} \rho_N \left[\ln \rho_N v - \ln Z_N - 1 - \beta \mu^{\mathrm{p}} N \right] \end{aligned} \tag{8.21}$$

The partition function of a polymer is given by[9]

$$Z_N = Z_1 \lambda^{N-1} \exp(-\beta\epsilon(N-1)) \tag{8.22}$$

where ϵ is the energy associated with a bond between two monomers, Z_1 is the partition function of a monomer, and λ is a non-universal model-dependent parameter that relates to the bending stiffness of the supramolecular chain. Substituting Eq. 8.22 into Eq. 8.21 gives

$$\begin{aligned}
\frac{\beta\,\Omega}{V} &= \sum_{N=1}^{\infty} \rho_N \left[\ln \rho_N v - \ln Z_1 - (N-1)\ln\lambda + (N-1)\beta\epsilon - 1 - \beta\mu^{\mathrm{p}} N\right] \\
&= \sum_{N=1}^{\infty} \rho_N \left[\ln \rho_N v - \ln Z_1 + \ln\lambda - \beta\epsilon + N(\beta\epsilon - \beta\mu^{\mathrm{p}} - \ln\lambda) - 1\right] \\
&= \sum_{N=1}^{\infty} \rho_N \left[\ln \rho_N v + \beta G + \beta\tilde{\mu} N - 1\right]
\end{aligned} \tag{8.23}$$

where we have defined an effective free energy per bond G, and an effective chemical potential per particle $\tilde{\mu}$

$$\beta G = -\ln Z_1 + \ln\lambda - \beta\epsilon, \quad \beta\tilde{\mu} = \beta\epsilon - \beta\mu^{\mathrm{p}} - \ln\lambda \tag{8.24}$$

At equilibrium $\partial\Omega/\partial\rho_N = 0$, namely

$$\frac{\beta}{V}\frac{\partial\Omega}{\partial\rho_N} = \ln \rho_N v + \beta G + \beta\tilde{\mu} N = 0 \tag{8.25}$$

and so the density ρ_N of N-mers at equilibrium is

$$\rho_N = \frac{\exp(-\beta\tilde{\mu}N)}{v\exp(\beta G)} = \frac{\exp(-\beta\tilde{\mu}N)}{2\Delta}, \tag{8.26}$$

where for convenience we have defined

$$\Delta \equiv \frac{v}{2}\exp(\beta G). \tag{8.27}$$

The effective chemical potential $\tilde{\mu}$ can be calculated from the total density (Eq. 8.10)

$$\rho = \sum_{N=1}^{\infty} N\rho_N = \frac{1}{2\Delta}\sum_{N=1}^{\infty} N \exp(\beta\tilde{\mu})^{-N} \tag{8.28}$$

$$= \frac{1}{2\Delta}\frac{\exp(\beta\tilde{\mu})}{(\exp(\beta\tilde{\mu}) - 1)^2} \tag{8.29}$$

from which $\exp(\beta\tilde{\mu})$ can be written as

$$\exp(\beta\tilde{\mu}) = \frac{1 + 4\rho\Delta + \sqrt{1 + 8\rho\Delta}}{4\rho\Delta} \tag{8.30}$$

Analogously the average cluster length $\bar{N}$ can be calculated:

$$\bar{N} = \frac{\sum_{N=1}^{\infty} N\rho_N}{\sum_{N=1}^{\infty} \rho_N} = \frac{\sum_{N=1}^{\infty} N \exp(\beta\tilde{\mu})^{-N}}{\sum_{N=1}^{\infty} \exp(\beta\tilde{\mu})^{-N}} = \frac{\exp(\beta\tilde{\mu})}{\exp(\beta\tilde{\mu}) - 1} \tag{8.31}$$

By substituting Eq.8.30 into Eq.8.31 we arrive at

$$\bar{N} = \frac{1}{2} + \frac{1}{2}\sqrt{1 + 8\rho\Delta} \tag{8.32}$$

Finally, from Eqs.8.26, 8.30 and 8.32 we can calculate the distribution of cluster lengths ρ_N

$$\rho_N = \frac{1}{2\Delta}\left(\frac{\bar{N} - 1}{\bar{N}}\right)^N = \frac{\rho}{\bar{N}(\bar{N} - 1)}\left(\frac{\bar{N} - 1}{\bar{N}}\right)^N \tag{8.33}$$

We can get the values of the available bonding volume v, and the effective free energy per bond G from simulations, by measuring $\bar{N}$ as a function of the inverse temperature β. From Eq. 8.32 we can see that

$$\rho\Delta = \frac{1}{2}\rho v \exp(\beta G) = \frac{1}{2}\bar{N}(\bar{N} - 1) \quad \Rightarrow \quad \ln\left(\bar{N}(\bar{N} - 1)\right) = \log \rho v + \beta G \tag{8.34}$$

8.A.3 The chemical potential, the pressure and the ideal limits

When we substitute Eq. 8.26 into Eq. 8.23, and use the definitions Eqs. 8.28 and 8.31 to evaluate the sum, we obtain

$$\Omega = \frac{V}{\beta}\sum_{N=1}^{\infty} -\rho_N = -\frac{M}{\beta\bar{N}} \tag{8.35}$$

The free energy is

$$F = \Omega + \mu^{\mathrm{p}} M \tag{8.36}$$

where μ^{p} can be derived from Eqs. 8.24, 8.31 and 8.32

$$\mu^{\mathrm{p}} = -\beta^{-1}\left(\beta\tilde{\mu} + \beta G + \ln Z_1\right) = -\beta^{-1}\left(\beta\tilde{\mu} + \log\left(\frac{2\Delta}{v}\right) + \ln Z_1\right) \tag{8.37}$$

$$= -\beta^{-1}\left[\ln\left(\frac{\bar{N}}{\bar{N} - 1}\right) + \ln\left(\frac{\bar{N}(\bar{N} - 1)}{\rho v}\right) + \ln Z_1\right] \tag{8.38}$$

$$= \beta^{-1}\log(\rho v) - \beta^{-1}\left[2\ln\bar{N} + \ln Z_1\right]. \tag{8.39}$$

Notice that the first term on the right hand side of Eq. 8.39 is the chemical potential of an ideal gas of point particles. The free energy can be calculated from the chemical potential and the grand potential

$$F = \Omega + \mu^{\mathrm{p}} M = -\frac{M}{\beta}\left\{\frac{1}{\bar{N}} - \log(\rho v) + 2\ln\bar{N} + \ln Z_1\right\} \tag{8.40}$$

For this solution the equality holds that

$$\mu^{\mathrm{p}} = \frac{\partial F}{\partial M}, \tag{8.41}$$

where we use the fact that both $\bar{N}$ and ρ are functions of M.

The pressure is defined as

$$P = -\frac{\partial F}{\partial V} \tag{8.42}$$

where $\bar{N}$ is a function of the volume. However, an easier way to calculate the pressure is by noting that for an ideal gas

$$P_{\mathrm{id}} = \frac{1}{\beta}\sum_{N=1}^{\infty}\rho_N = \frac{\rho}{\beta\bar{N}} \tag{8.43}$$

It is easy to check that the pressures of Eqs. 8.42 and 8.43 are equal by substituting Eq. 8.32 into Eq.8.40 and writing $\rho = M/V$.

We note that this model behaves like an ideal gas of point particles in the limit $\lim_{\rho\to 0}\bar{N} = 1$, so

$$\lim_{\rho\to 0}\Omega = -\frac{M}{\beta} \qquad \lim_{\rho\to 0}\mu^{\mathrm{p}} = \mu^{\mathrm{m}} - \beta^{-1}\log(\rho v) \tag{8.44}$$

$$\lim_{\rho\to 0}P = \frac{\rho_t}{\beta} \qquad \lim_{\rho\to 0}F = -\frac{M}{\beta} + \frac{M}{\beta}\log(\rho v) \tag{8.45}$$

where we have used that $Z_1 = 1$ for ideal point particles, and introduced μ^{m} as the chemical potential of an ideal gas.

Appendix 8.B Ideal polymer sublimation

In this section we will derive a qualitative phase diagram for the bundling of an ideal polymer gas. For this purpose we equate the chemical potential of a particle in the Ideal Free Association (IFA) model of Section 8.A to the chemical potential of a particle in an Einstein crystal. We assume that the particles do not have any internal degrees of freedom, and so $Z_1 = 1$.

8.B.1 The Einstein crystal

We assume an infinite Einstein crystal. The energy of one particle in the solid is then given by

$$U_i = \frac{1}{2}kx^2 + \frac{1}{2}ky^2 + \frac{1}{2}kz^2 - \epsilon_{\text{sol}} \tag{8.46}$$

where k is the spring constant of the harmonic potential and $-\epsilon_{\text{sol}}$ is the energy of a particle at the origin of its harmonic potential. This harmonic potential is an effective potential to describe the many pair potentials in the solid, so that we can separate the individual components in the partition function

$$\begin{aligned} Q_{\text{sol}} &= \Lambda^{-3M} \int \prod_i^M \exp(-\beta U_i) d^3r_1 \cdots d^3r_M \\ &= v^{-M} \left(\int \exp\left[-\beta \left(\frac{1}{2}kx^2 + \frac{1}{2}ky^2 + \frac{1}{2}kz^2 + \epsilon_{\text{sol}} \right) \right] dxdydz \right)^M \\ &= \left(\frac{\exp\left[\beta\epsilon_{\text{sol}}\right]}{v} \left(\frac{2\pi}{\beta k} \right)^{\frac{3}{2}} \right)^M \equiv \exp\left[-\beta\mu_{\text{sol}}\right]^M \end{aligned} \tag{8.47}$$

Where the de Broglie wavelength is taken as the available bonding volume $v \equiv \Lambda^3$, as already done in Section 8.A for the IFA-model. The free energy is defined as

$$F_{\text{sol}} = -\frac{1}{\beta} \ln Q = -M\epsilon_{\text{sol}} + \frac{M}{\beta} \log \left[v \left(\frac{\beta k}{2\pi} \right)^{\frac{3}{2}} \right] \tag{8.48}$$

The chemical potential is then simply

$$\mu_{\text{sol}} = \frac{\partial F}{\partial M} = -\epsilon_{\text{sol}} + \frac{1}{\beta} \log \left[v \left(\frac{\beta k}{2\pi} \right)^{\frac{3}{2}} \right] \tag{8.49}$$

At sublimation, the chemical potential of the polymer gas (Eq. 8.39) (with $Z_1 = 1$) and the solid (Eq. 8.49) should be equal, giving us an expression for the density ρ of the gas as a function of temperature, at the gas-solid binodal

$$\mu^{\text{p}} = \mu_{\text{sol}}$$

$$\frac{1}{\beta}\log(\rho v) - \frac{2}{\beta}\log\bar{N} = -\epsilon_{\text{sol}} + \frac{1}{\beta}\log\left[v \left(\frac{\beta k}{2\pi} \right)^{\frac{3}{2}} \right] \tag{8.50}$$

$$\frac{4\rho}{\left(1 + \sqrt{1 + 8\rho\Delta}\right)^2} = \left(\frac{\beta k}{2\pi} \right)^{\frac{3}{2}} \exp(-\beta\epsilon_{\text{sol}}) \tag{8.51}$$

In the ideal gas limit $\Delta = 0$ (i.e. $\bar{N} = 1$) we get the sublimation line $\rho^{\mathrm{m}}_{\mathrm{sub}}$ of an ideal gas of point particles in coexistence with an Einstein crystal

$$\rho^{\mathrm{m}}_{\mathrm{sub}} = \left(\frac{\beta k}{2\pi}\right)^{\frac{3}{2}} \exp(-\beta\epsilon_{\mathrm{sol}}) \tag{8.52}$$

and so for a gas of polymers the sublimation line is given by $\rho^{\mathrm{p}}_{\mathrm{sub}}$

$$\frac{4\rho^{\mathrm{p}}_{\mathrm{sub}}}{\left(1+\sqrt{1+8\rho^{\mathrm{p}}_{\mathrm{sub}}\Delta}\right)^2} = \rho^{\mathrm{m}}_{\mathrm{sub}} \tag{8.53}$$

$$\rho^{\mathrm{p}}_{\mathrm{sub}} = \frac{\rho^{\mathrm{m}}_{\mathrm{sub}}}{\left(2\rho^{\mathrm{m}}_{\mathrm{sub}}\Delta - 1\right)^2} \tag{8.54}$$

In the IFA-model $\Delta \equiv v\exp(\beta G)/2$ and in that case

$$\rho^{\mathrm{p}}_{\mathrm{sub}} = \frac{\rho^{\mathrm{m}}_{\mathrm{sub}}}{\left(v\left(\frac{\beta k}{2\pi}\right)^{\frac{3}{2}}\exp[\beta(G-\epsilon_{\mathrm{sol}})]-1\right)^2}. \tag{8.55}$$

The polymer sublimation line $\rho^{\mathrm{p}}_{\mathrm{sub}}$ will approach the ideal gas sublimation line $\rho^{\mathrm{m}}_{\mathrm{sub}}$ when $\epsilon_{\mathrm{sol}} \gg G$, i.e. when the energy gain of deposition – the opposite of sublimation – far exceeds the gain of polymerization.

8.B.2 The Wertheim thermodynamic perturbation theory

For realistic bond potentials the energy of a bond changes with the distance and orientation of the particles, and is not a constant ϵ as in the IFA-model. The temperature of the system determines the average energy per a bond, which for a harmonic potential is equal to $k_BT/2$ per degree of freedom, and so the average effective free energy per bond will also decrease with temperature. In the expression $\Delta = v\exp(\beta G)/2$ the terms v and G will be temperature dependent for such spatially varying potentials.

The Wertheim Thermodynamic Perturbation Theory (WTPT), applied to the case of equilibrium polymerization, refines the IFA-expression by redefining Δ of equation 8.27 as $\Delta = \Delta^W$[2]

$$\Delta^{\mathrm{W}} \equiv 4\pi \int g_{\mathrm{rep}}(r)\left\langle \exp(-\beta V_{\mathrm{att}}(r)) - 1\right\rangle_{\omega_1,\omega_2} r^2 dr, \tag{8.56}$$

where Δ^{W} involves a single site-site interaction, $V_{\mathrm{att}}(r)$ is the attractive part of the pair potential, $\langle . \rangle_{\omega_1,\omega_2}$ denotes an average over all orientations ω_1 and ω_2 of the two molecules, and $g_{\mathrm{rep}}(r)$ is the pair correlation function of the repulsive part of the potential. Eq. 8.56 assumes that no rings are formed, and that the potential can clearly be separated into an attractive and a highly repulsive part. Note that Eq. 8.56 is very similar to the expression for the second virial coefficient.

It is easy to see that Δ^W resembles Δ of the IFA-expression for low densities, where $g_{\text{rep}}(r) \approx 1$. In principle the IFA-model describes a square well patchy particle with bond energy ϵ and available bonding volume per particle v. Sciortino et al. showed that in that case[2]

$$\Delta^{\text{W}} \approx V_b[\exp(\beta\epsilon) - 1] \approx \frac{v}{2}\exp(\beta\epsilon) \tag{8.57}$$

where the approximation holds when $\beta \gg \epsilon$, and where V_b is the spherically averaged bonding volume of a single bond (whereas v is the available bonding volume for a single particle). For simple geometries V_b can be calculated analytically. For example, spherical square well patches of radius δ, with the center at the surface of a hard sphere of radius σ, have an average bonding volume of[2]

$$V_b = \frac{\pi\delta^4\,(15\sigma + 4\delta)}{30\sigma^2}. \tag{8.58}$$

For realistic potentials Δ^{W} has to be determined numerically. In this chapter we always use the ideal gas approximation $g_{\text{rep}}(r) = 1$, because our simulations are done at relatively low densities. Evaluating Eq. 8.56 requires the integration of the pair potential over seven degrees of freedom (integration over ω_1 and ω_2 both represent three degrees of freedom, r represents one), and we therefore use Monte Carlo integration, as it is the best method for integrating over higher dimensional spaces. To this purpose we place a particle with one patch at the center of a cubic box in a random orientation, and place a second particle with the same type of patch at a random position within the box, and with a random orientation. The volume V is chosen so that if the second particle is positioned at the edge of the box, it cannot interact with the particle at the origin. Each consecutive step we assign a random orientation to both particles, move the second particle to a random position inside the box, and calculate the value of the interaction potential V_i. We then determine the attractive contribution $V_{\text{att},i}$ as

$$V_{\text{att},i} = \begin{cases} V_i & \text{if } V_i < 0 \\ 0 & \text{if } V_i \geq 0 \end{cases} \tag{8.59}$$

The value of Δ^W is then easily calculated simultaneously for a range of temperatures

$$\Delta_i^{\text{W}}(\beta) = \frac{i-1}{i}\Delta_{i-1}^{\text{W}}(\beta) + \frac{V}{i}\left[\exp(-\beta V_{\text{att},i}) - 1\right] \tag{8.60}$$

with $\Delta_0^{\text{W}} = 0$, and starting at $i = 1$.

Appendix 8.C The bending rigidity of a polymer chain

The bending rigidity κ of a rod is defined by the bending energy E_{bend} as[8]

$$E_{\text{bend}} = \frac{\kappa}{2}\int_0^L \frac{1}{R(s)^2} ds$$

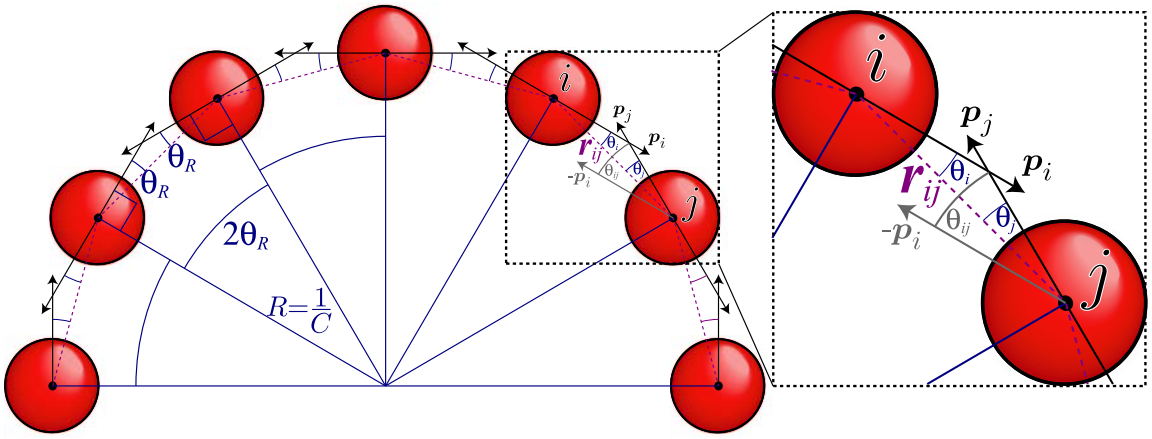

Figure 8.5: Set-up used to calculate the bending rigidity of a polymer chain. Place patchy particles on a circle of radius $R = 1/C$, where C is the curvature. Place the particles a distance $r_{ij} = 2^{\frac{1}{6}}\sigma$ apart, with the patches directed along the tangent of the circle. In the inset the definition of the angles θ_i, θ_j and θ_{ij} are given, used in Eq. 8.1 to calculate the potential between patch i and patch j. In this configuration $\theta_i = \theta_j = \theta_{ij}/2 = \theta_R$, where θ_R is given in Eq. 8.62

where $R(s)$ is the radius along the path at position s. If we bend the rod in exactly the same way along its length, i.e. into a semi-circular shape with curvature C, then E_{bend} becomes

$$E_{\text{bend}} = \frac{\kappa}{2}\int_0^L C^2 ds = \frac{\kappa}{2}C^2 L$$

This can be discretized for a polymer of $N+1$ particles, i.e. with N bonds, as

$$E_{\text{bend}} = \frac{\kappa}{2}\sum_{i=1}^{N} C^2\Delta L = \frac{\kappa}{2}NC^2\Delta L = N\Delta E \;\Rightarrow\; \kappa = \lim_{C\to 0}\frac{2\Delta E}{C^2\Delta l} \tag{8.61}$$

where Δl is the distance of a bond and ΔE is the bending energy of a single polymer bond. The limit is taken because in practice $\Delta E/C^2$ is not a constant.

For the chains used in this chapter, i.e. for a chain of spherical beads with two exactly opposing, attractive patches of the type defined in Eq. 8.1 and Fig. 8.1, ΔE is defined in Fig. 8.5 as

$$\begin{aligned}\Delta E &= V(2^{1/6}\sigma, \theta_R, \theta_R, 2\theta_R) - V(2^{1/6}\sigma, 0, 0, 0), \quad \theta_R = \arcsin\left(\frac{2^{1/6}\sigma C}{2}\right)\\ &= \epsilon\left\{1 - \exp\left[-\frac{3}{2w^2}\arcsin\left(\frac{2^{1/6}\sigma C}{2}\right)\right]\right\}\end{aligned} \tag{8.62}$$

where $\Delta l = 2^{1/6}\sigma$ is the equilibrium separation of a bond. Finally, substituting ΔE in Eq.8.61, and expanding it around $C = 0$, gives the bending rigidity of the patchy

polymer chain

$$\kappa = \lim_{C\to 0} \frac{3\epsilon 2^{1/6}\sigma}{4w^2} + \frac{\epsilon\sqrt{2}\sigma^3\left(4w^2-9\right)}{64w^4}C^2 + \mathcal{O}(C^4) = \frac{3\epsilon 2^{1/6}\sigma}{4w^2} \tag{8.63}$$

Appendix 8.D Quaternions, and their use in Monte Carlo simulations

Quaternions are an extension of complex numbers, and, when properly normalized, are a very convenient way to describe the orientation of an object in three-dimensional space. This is because their four coordinates map exactly onto a three-dimensional rotation matrix, and because this representation does not have the singularities that are characteristic of for instance the Euler angle representation. In Monte Carlo simulations they offer an efficient and simple way to perform rotational moves of molecules and of the clusters they form[13].

A complex number is defined as $c = a + bi$, where $i^2 = -1$ and $a, b \in \mathbb{R}$. The quaternion has two extra coordinates

$$q = q_0 + q_1 i + q_2 j + q_3 k,\ q_0, q_1, q_2, q_3 \in \mathbb{R} \tag{8.64}$$

subject to the rules

$$i^2 = j^2 = k^2 = ijk = -1. \tag{8.65}$$

From these rules all the sum and product rules can be derived, such as $ij = k$, $jk = i$, $ki = j$, $ji = -k$, $kj = -i$, and $ik = -j$. A quaternion q has a conjugate q^* defined as

$$q^* = q_0 - q_1 i - q_2 j - q_3 k. \tag{8.66}$$

Addition and multiplication of the two quaternions $q = (q_0, q_1, q_2, q_3)$ and $p = (p_0, p_1, p_2, q_3)$ are therefore given as follows

$$p + q = (q_0 + p_0) + (q_1 + p_1)i + (q_2 + p_2)j + (q_3 + p_3)k \tag{8.67}$$

$$\begin{aligned} pq =& (q_0p_0 - q_1p_1 - q_2p_2 - q_3p_3) + (q_0p_1 + q_1p_0 + q_2p_3 - q_3p_2)i \\ &+ (q_0p_2 - q_1p_3 + q_2p_0 + q_3p_1)j + (q_0p_3 + q_1p_2 - q_2p_1 + q_3p_0)k. \end{aligned} \tag{8.68}$$

With these results we can calculate the length, or norm, of a quaternion

$$n(q) = \sqrt{qq^*} = \sqrt{q^*q} = \sqrt{q_0^2 + q_1^2 + q_2^2 + q_3^2}, \tag{8.69}$$

and a quaternion is normalized when $\sqrt{qq^*} = 1$. With this the inverse of the quaternion q^{-1} can be calculated

$$q^{-1} = \frac{q^*}{qq^*} \tag{8.70}$$

and division is possible, as it is simply the multiplication with the inverse of the other quaternion. The quaternion can be interpreted as having a scalar, and a vector part

$$q = q_0 + \vec{q}_v, \quad \vec{q}_v = (q_1, q_2, q_3) \tag{8.71}$$

so that quaternion multiplication can be written as

$$pq = q_0 p_0 - \vec{q}_v \cdot \vec{p}_v + [q_0 \vec{p}_v + p_0 \vec{q}_v + \vec{q}_v \times \vec{p}_v] \tag{8.72}$$

where the part in front of the square brackets is a scalar, and the part inside the square brackets a vector. If the quaternion is normalized this representation can also be written as

$$q = \cos\left(\frac{\alpha}{2}\right) + \sin\left(\frac{\alpha}{2}\right)\hat{n}, \quad \alpha \in \mathbb{R} \tag{8.73}$$

where α is a scalar representing an angle and $\hat{n} = (\hat{n}_x, \hat{n}_y, \hat{n}_z)$ is a normalized 3-vector, representing a rotation-axis. If we write a point in 3D-space $\vec{p}$ as a quaternion $p = (0, \vec{p})$ then rotation by an angle α around the vector $\hat{n}$ can be performed by

$$p' = qpq^{-1} = qpq^* \tag{8.74}$$

where the conjugate of q is equal to the inverse because q is normalized. In practice it is fastest to first create a rotation matrix M from the quaternion q, and multiply $\vec{p}$ by this matrix, i.e. $p' = M\vec{p}$ with M

$$M = \begin{pmatrix} q_0^2 + q_1^2 - q_2^2 - q_3^2 & 2q_1q_2 - 2q_0q_3 & 2q_0q_2 + 2q_1q_3 \\ 2q_0q_3 + 2q_1q_2 & q_0^2 - q_1^2 + q_2^2 - q_3^2 & 2q_1q_3 - 2q_0q_1 \\ 2q_1q_3 - 2q_0q_2 & 2q_0q_1 + 2q_2q_3 & q_0^2 - q_1^2 - q_2^2 + q_3^2 \end{pmatrix} \tag{8.75}$$

At first sight, quaternions seem rather complex for describing spatial orientations of e.g. molecules in a Monte Carlo simulation. After all, in the end we still have to generate a rotation matrix to multiply our points with. We could just as well have generated this matrix from an angle and a rotation vector, or from Euler angles. However, to generate a rotation matrix from Euler angles one has to calculate three sines and three cosines which are computationally expensive operations. Also, one needs one sine and one cosine to generate the rotation matrix for a rotation vector and rotation angle pair. Performing multiple rotations consecutively on the same point in space is also much cheaper using quaternions than using matrix multiplications. Furthermore, not all three angles of the Euler angles are equal. One starts with a rotation around the first Euler angle, then a rotation around a perpendicular axis by the second angle, completed by a third rotation around the last perpendicular axis. This can cause gimbal lock, in which the change of one of the angles cannot change the orientation of the object anymore.

Euler angles ϕ, θ and ψ can easily be transformed to a quaternion by

$$\begin{aligned} q = &\cos\left(\frac{\phi+\psi}{2}\right)\cos\left(\frac{\theta}{2}\right) + \cos\left(\frac{\phi-\psi}{2}\right)\sin\left(\frac{\theta}{2}\right) i \\ &+ \sin\left(\frac{\phi-\psi}{2}\right)\sin\left(\frac{\theta}{2}\right) j + \sin\left(\frac{\phi+\psi}{2}\right)\cos\left(\frac{\theta}{2}\right) k \end{aligned} \tag{8.76}$$

8.D.1 Randomizing quaternions

It is very easy to generate a random orientation with quaternions, in such a way that each orientation has an equal probability. One just has to generate points uniformly distributed on the surface of a 4D-sphere of radius 1

```
do
{ x0=2*ran()-1; x1=2*ran()-1;
} while ( (S1=x0*x0+x1*x1)>1)
do
{ x2=2*ran()-1; x3=2*ran()-1;
} while ( (S2=x2*x2+x3*x3)>1)
len=sqrt((1-S1)/S2);
q0=x0; q1=x1; q2=x2*len; q3=x3*len;
```

where `ran()` returns a uniform random number in the interval $[0, 1]$.

Using quaternions it is also very easy to change the orientation of a molecule by a small amount δq. The easiest way is to generate a random point δq inside a 4D-sphere of radius $\delta q_{\max}$ (`dqmax`), for instance in the following way

```
do
{ q0=2*ran()-1; q1=2*ran()-1;q2=2*ran()-1; q3=2*ran()-1;
} while ( (norm2=q0*q0+q1*q1+q2*q2+q3*q3)>1)
q0=q0*dqmax;q1=q1*dqmax;q2=q2*dqmax;q3=q3*dqmax;
```

Then simply add the random quaternion to the orientation $q' = q + \delta q$, and normalize q' to get a new, slightly different, orientation.

Adding unnormalized quaternions and normalizing the resulting quaternion is only useful for changing the orientation of a single molecule with respect to e.g. its center of mass. To rotate a cluster of molecules around a fixed line through the center of mass of the cluster by a small amount δq, we cannot use the advantages of the quaternion and we have to generate the axis and the angle randomly. The rotation vector is generated by creating points on a 3D-sphere of radius 1, and the angle α is a random, small scalar. Eq. 8.73 can then be used to determine the rotation quaternion. First translate all the molecules of the cluster to the center of mass frame of reference, then multiply both the position and the orientational quaternion of the molecule by δq, and then translate the molecules of the cluster back to the box coordinate system.

8.D.2 Reptation moves

Reptation moves are a way to speed up the equilibration of the polymer chain length distribution during Monte Carlo simulations. During a reptation move you remove a molecule from one randomly chosen end of a randomly chosen chain, and attach it to another randomly chosen end of another randomly chosen chain. If detailed balance is preserved and the Boltzmann criterion is met, then the move is accepted.

Detailed balance can only be preserved if the number of clusters is not changed by the move. You must therefore always check if the addition of the molecule to the end of a chain does not couple two clusters together according to your cluster criterion. In practice this is most easily confirmed by checking whether the new cluster size is the old cluster size plus one. Detailed balance also dictates that it should be possible to perform the reverse move in the exact opposite way as the forward move. For this reason the orientation of the molecule with respect to its old and new neighbors should be very well defined. And this is again very conveniently done with quaternions, or rotation matrices.

The problem is as follows. Say that r_n is the position and q_n the orientation of a particle at the end of a polymer, and r_{n-1} and q_{n-1} are the position and orientation of its only neighbor. Now we wish to move this particle to the end of another polymer, so that it gets a new position r_m and orientation q_m, and a new neighbor with position r_{m-1} and orientation q_{m-1}. We must choose r_m and q_m in such a way that if we do the reverse move, i.e. take the particle from its new neighbor, and move it to its old neighbor, it ends up at r_n with orientation q_n. This is the case if we choose

$$q_m = q_{m-1} q_{n-1}^{-1} q_n \tag{8.77}$$

i.e. we take the orientation of particle n, transform it to the coordinate system of particle $n-1$, and rotate it by the orientation of the new neighbor. Performing the reverse move then gives the old orientation again

$$q_n = q_{n-1} q_{m-1}^{-1} q_m = q_{n-1}(q_{m-1}^{-1} q_{m-1}) q_{n-1}^{-1} q_n = (q_{n-1} q_{n-1}^{-1}) q_n = q_n. \tag{8.78}$$

The position is chosen in a similar way,

$$r_m = r_{m-1} + P\Delta r_{new} = r_{m-1} + P[q_{m-1} q_{n-1}^{-1}(r_n - r_{n-1})] \tag{8.79}$$

where P is randomly chosen to be $+1$ or -1 when the second cluster is a monomer, and where P assures that the new position is correctly placed at the end, if the second cluster is a polymer, i.e. the particle is positioned in approximately the same direction as $r_{m-1} - r_{m-2}$,

$$P = \text{sign}[\Delta r_{new} \cdot (r_{m-1} - r_{m-2})] \tag{8.80}$$

again, the reverse move is

$$\begin{aligned} r_n &= r_{n-1} + P_2[q_{n-1} q_{m-1}^{-1}(r_m - r_{m-1})] && (8.81)\\ &= r_{n-1} + P_2[q_{n-1} q_{m-1}^{-1}(r_{m-1} + P_1[q_{m-1} q_{n-1}^{-1}(r_n - r_{n-1})] - r_{m-1})] \\ &= r_{n-1} + P_1 P_2[q_{n-1} q_{m-1}^{-1}[q_{m-1} q_{n-1}^{-1}(r_n - r_{n-1})]] \\ &= r_{n-1} + P_1 P_2(r_n - r_{n-1}) \\ &= P_1 P_2 r_n && (8.82) \end{aligned}$$

where $P_1 P_2 = 1$.

8.1 References

[1] R. F. Service. Science **309**, 95 (2005).

[2] F. Sciortino, E. Bianchi, J. F. Douglas, P. Tartaglia. J. Chem. Phys. **126**, 194903 (2007).

[3] A. W. Wilber, et al. J. Chem. Phys. **127**, 085106 (2007).

[4] Z. Zhang, A. S. Keys, T. Chen, S. C. Glotzer. Langmuir **21** 11547 (2005).

[5] H. Engelkamp, S. Middelbeek, and R. J. M. Nolte. Science **284**, 785 (1999).

[6] P. Jonkheijm, P. van der Schoot, A. P. H. J. Schenning, E. W. Meijer. Science **313**, 80 (2006).

[7] L. Brunsveld et al. Proc. Nat. Acad. Sci. U. S. A **99**, 4977 (2002).

[8] C. P. Lowe. Phil. Trans. R. Soc. Lond. B **358** 1543 (2003).

[9] P. van der Schoot, in *Theory of Supramolecular Polymerization*, edited by A. Ciferri, Supramolecular Polymers, 2nd Ed. (CRC Press, Boca Raton, FL, 2005).

[10] M. Wertheim, J. Stat. Phys. **35**, 19 (1984); **35**, 35 (1984); **42**, 459 (1986).

[11] G. M. Grason and R. F. Bruinsma. Phys. Rev. Lett. **99**, 098101 (2007).

[12] D. Frenkel and A. J. C. Ladd. J. Chem. Phys. **81**, 3188 (1984).

[13] F. J. Vesely. J. of Comp. Phys. **47**, 291 (1982).